Journal of Surgery
Stepanova Yu A, et al. J Surg 11: 11584
www.doi.org/10.29011/2575-9760.11584
www.gavinpublishers.com
Research Article

Evaluation of The Effectiveness of Malignant Liver Tumor Cryodestruction Based on Electron Microscopic Data of Early Ultrastructural Changes in The Tumor, Taking into Account Various Models of Changes Depending on The Tumor Histogenesis

Stepanova Yu A[1], Chekmareva I A[1], Ionkin D A[1], Paklina OV[1], Bugaev SA[1], Chzhao AV[2]

[1]A.V. Vishnevsky National Medical Research Center of Surgery, Moscow, Russia

[2]JSC "Clinic K+31", Lobachevsky St., 42, building 4, 121354, Moscow, Russia

***Corresponding Author:** Stepanova Yulia Aleksandrovna, ultrasound diagnostics department, A.V. Vishnevsky National Medical Research Center of Surgery, st. B. Serpukhovskaya, 27, 115993, Moscow, Russia

Citation: Stepanova Yu A, Chekmareva I A, Ionkin D A, Paklina O V, Bugaev S A, et al. (2026) Evaluation of The Effectiveness of Malignant Liver Tumor Cryodestruction Based on Electron Microscopic Data of Early Ultrastructural Changes in The Tumor, Taking into Account Various Models of Changes Depending on The Tumor Histogenesis. J Surg 11: 11584DOI: 10.29011/2575-9760.011584.

Received Date: 11 March 2026; **Accepted Date:** 17 March 2026; **Published Date:** 19 March 2026

Abstract

Aim: to develop a method for assessing the effectiveness of malignant liver tumors destruction (hepatocellular carcinoma (HCC), cholangiocellular carcinoma (CCC), colorectal cancer metastasis (CRCM) after cryotherapy based on an electron microscopic study datas of early ultrastructural changes in tumors, taking into account various models of changes depending on the neoplasm histogenesis.

Materials and Methods: Electron microscopy was used to evaluate early ultrastructural changes in malignant liver tumors (HCC, CCC and CRCM) in patients operated on at A.V. Vishnevsky National Medical Research Center of Surgery. The study included 14 cases: HCC - 5, CCC - 4, CRCM - 5. Patients with a tumor size of 40±2.5 mm were selected for the study. Cryodestruction was performed in the presence of recurrence or metastases after a previous liver resection.

Study Methodology: Following a traditional laparotomy approach, the affected liver lobe was mobilized. A tissue biopsy of the tumor lesion was performed. Tumor tissue fragments were collected from the tumor center and from liver tissue along the tumor periphery. Cryodestruction was then performed. Two active freezing applications were performed with exposures of 3 and 1 min. After each application, the cryoapplicator was removed from the tumor tissue, and further warming of the destruction zone occurred spontaneously. During all stages of cryodestruction, intraoperative ultrasound was performed to guide and monitor the process. After the thermal exposure stage, a repeat biopsy of the lesion was performed to monitor the results. Tumor tissue fragments were collected from the tumor center and from liver tissue along the periphery of the cryotherapy-treated tumor. The obtained material was delivered as quickly as possible to the pathology department without formalin treatment for subsequent electron microscopic examination of the tumor and its microenvironment. This included morphometric analysis of the tumor, assessing the mitochondrial area in tumor cells before and after cryodestruction at the ultrastructural level, and identifying telocytes with subsequent determination of the

Citation: Stepanova Yu A, Chekmareva I A, Ionkin D A, Paklina O V, Bugaev S A, et al. (2026) Evaluation of The Effectiveness of Malignant Liver Tumor Cryodestruction Based on Electron Microscopic Data of Early Ultrastructural Changes in The Tumor, Taking into Account Various Models of Changes Depending on The Tumor Histogenesis. J Surg 11: 11584DOI: 10.29011/2575-9760.011584.

average number of telocyte-secreted microvesicles per 1 μm2 of extracellular matrix, as well as the extracellular matrix area (μm2).

Conclusion: A method for assessing the effectiveness of malignant liver tumor destruction following cryodestruction based on electron microscopic data has been developed. Electron microscopic examination of malignant liver tumor cells (HCC, BCC, and BCC) and the tumor microenvironment before and after cryodestruction allowed for the pathogenetic justification of a malignant tumor treatment regimen, confirming the tumor's destructive effect at the ultrastructural level.

Keywords: CCC; Cryodestruction; Colorectal cancer metastases; Electron microscopic study; HCC; Malignant liver tumors; Mitochondria; Telocytes; Tumor microenvironment; Ultrastructure

Introduction

Surgical treatment of malignant liver tumors is a complex task. Surgical intervention can lead to various intra- and postoperative complications. Although radical tumor removal by traditional surgery is considered the method of choice, it may be contraindicated in some patients [1,2]. Local thermal destruction methods for malignant liver tumors have become an alternative for patients with contraindications to traditional surgery. Such treatment methods include radiofrequency ablation, laser ablation, microwave ablation, alcoholization (chemical ablation), chemoembolization, and tumor cryodestruction. The use of cryodestruction as an alternative method for treating focal liver lesions began in the 1970s, when K. Stucke began using cold exposure to treat liver alveococcosis [3]. Subsequently, cryodestruction became widely used in the treatment of primary and metastatic liver lesions [4,5].

A significant contribution to the understanding of the physiology of cryotherapy was made by the Japanese researcher, one of the founders of the fundamental study of the effects of low temperatures, Sajio Sumida [6]. "Freezing with liquid nitrogen, due to its extremely low temperature, does not allow malignant cells to spread through the blood or lymphatic flow, or through the interstitial fluid...", i.e. they are blocked [7]. "Antigenic proteins released from malignant cells subjected to freezing activate the autoimmune system. Activation of both humoral and cellular immune responses occurs. Cryoimmunological destruction of the tumor can be enhanced when used in combination with biological response modifiers (BRMs) and traditional chemotherapy" [8].

Indications for cryodestruction in the treatment of malignant liver tumors include the impossibility of performing radical surgery due to the general condition of the patient; simultaneous resection of the contralateral liver lobe; previously performed liver resection (the volume of remaining parenchyma doesn't allow for repeat liver resection).

Currently, recommendations for the use of cryodestruction for the treatment of malignant liver tumors only focus on the size of the tumor being treated, with little consideration given to the tumor type. For example, in a meta-analysis of cryotherapy data for malignant liver tumors published after 2000 in the PubMed, Web of Science, Embase, and Scopus databases in accordance with the PRISMA guidelines, the morphology of the tumor wasn't a separate evaluation criterion. The intervention was performed based on the location, size, and number of the lesions, with these parameters being selected to determine the procedure protocol [9]. In general, in publications describing the treatment of malignant liver tumors using cryotherapy, the size of the lesions ranges from 1.0 to 13.5 cm, and the number of lesions ranges from 1 to 10 (4±3) [4,5,10-13]. The size of the lesion being treated also depends on the cryoapplicator used: for example, transhepatic applicators for puncture treatments use diameters ranging from 1.5 to 8 mm; applicators for cryodestruction during open surgery range from 8 mm to 5.0 cm.

Currently, there are two theories regarding the origin of cancer: the classical somatic mutation theory (SMT) and tissue organization field theory (TOFT) [14]. TOFT suggests that cancer arises as a result of disruption of the cellular microenvironment. According to this theory, exosomes secreted by tumor cells contain a multitude of different epigenetic molecules and a huge variety of proteins, including microRNAs and genomic DNA segments, which play a crucial role in the preparation of tumor metastatic niches. Telocytes also play an important role in the integration of intercellular interactions, both in health and disease. Telocytes are recently described as specialized stromal cells [15]-due to their very long cytoplasmic processes (60–100 μm) (telopodium), they form a dense network within organs and the body, communicating with many cell types through intercellular contacts, as well as by synthesizing various types of microvesicles and their intercellular exchange. Therefore, methods aimed at destroying not only the tumor cell but also its microenvironment are relevant and effective.

The microstructural features of various tumor cells suggest different responses from mitochondria, which have their own genome [16-18] that does not affect the entire cell. However, this local autonomy may impact the energy supply (survival) of a specific tumor morphological unit and, consequently, the results of cryotherapy.

According to N.V. Usoltseva and V.A. Usoltseva (1980), the physical structure of the tissue, in particular the ratio between

the volume of water contained within it, as well as the degree of development of the microcirculatory bed, largely determine the volume of freezing during cryotherapy on biological tissues [19]. V.V. Shafranov et al. (2017) identified the reasons for the limitations of cryogenic tissue destruction, namely, the density of the tissue structure and intensive metabolism, which determines a high level of heat generation and ultimately leads to the establishment of a steady state in the tissue volume [20]. As noted above, in malignant tumors, in addition to the proliferation and metastasis of tumor cells themselves, the microenvironment plays a significant role in tumor progression. In addition to the cellular elements of the tumor microenvironment, the extracellular matrix itself plays a significant role. It consists of proteins, proteoglycans, minerals, and water, as well as macromolecules such as collagens, glycoproteins, and enzymes that influence intercellular interactions, adhesion, and cell proliferation. The extracellular matrix, possessing the properties of a living cell, not only provides a scaffold for cells but also serves as a medium for active components secreted by tumor cells and cells of the microenvironment in free form, as well as in microvesicles and exosomes. The composition of stromal cells in the tumor microenvironment can vary significantly depending on the tumor type [21]. Determining the composition of the microenvironment of hepatocellular carcinoma (HCC), cholangiocellular carcinoma (CCC), colorectal cancer metastasis (CRCM) and its response to cryotherapy can also help in developing the most effective cryotherapy protocol depending on the nature of the tumor.

Previous studies of morphological changes in liver cells during cryodestruction have revealed structural and functional changes in hepatocytes and endothelial cells and their severity depending on the location of cryotherapy after liver resection [22]. Following the resection stage of planned liver surgery, patients underwent cryodestruction of the organ stump using a cryosurgical apparatus with a 2 cm diameter applicator. Prior to cryodestruction, intraoperative ultrasound (IOUS) of the tumor was performed to determine the center of the neoplasm. The cryogenic applicator was positioned in the projection of the tumor center, followed by cold exposure to the pathological lesion, extending the aforementioned effect to the liver parenchyma surrounding the tumor. The zone of primary early necrotic changes associated with the destruction of liver cells under the influence of low temperature was observed at a depth of up to 4 mm after a single freezing and up to 7 mm after two cryotherapy sessions along the margin of the liver resection. Direct exposure to low temperature led to necrosis of hepatocytes. Most cells were completely destroyed and represented cellular debris. The integrity of the hepatocyte plasma membrane was disrupted, making the cell boundaries virtually indistinguishable. Early after cryodestruction of the liver stump, the degree of tissue damage in the affected area depended on the depth of the tissue relative to the cryoapplicator and the repetition of freeze-thaw cycles. Cryodestruction increased with repeated freeze-thaw cycles.

In another study, the authors demonstrated that cryoinjury induces apoptosis in colorectal cancer liver metastasis cells by disrupting mitochondrial integrity [23]. However, all these studies do not take into account the morphology of tumors in the comparative aspect of assessing ultrastructural changes during cryodestruction, and also do not evaluate its microenvironment.

The aim: to develop a method for assessing the effectiveness of malignant liver tumors destruction (HCC, CCC and CRCM) after cryotherapy based on an electron microscopic study datas of early ultrastructural changes in tumors, taking into account various models of changes depending on the neoplasm histogenesis..

Materials and Methods

Electron microscopy was used to evaluate early ultrastructural changes in malignant liver tumors (HCC, CCC, and CRCM) in 14 patients undergoing surgery at A.V. Vishnevsky National Medical Research Center of Surgery. Patients with a tumor size of 40±2.5 mm were selected for the study. Cryosurgery was performed in the presence of recurrence or metastases after previous liver resection. Adjacent blood vessels and large bile ducts were not considered a contraindication to cryodestruction. The characteristics of the patients and malignant liver tumors are presented in Table 1.

№	Gender	Age (years)	Morphological diagnosis	Surgery
1	M	54	HCC	Left hemihepatectomy
2	F	58	CCC	Left caval lobectomy
3	M	61	HCC	Resection of V-VI-VII segments
4	F	72	CRCM	Resection of VI-VII segments
5	M	56	CRCM	Left hemihepatectomy
6	M	68	CRCM	Resection of V-VI segments
7	F	54	CCC	Left hemihepatectomy
8	M	51	CRCM	Left hemihepatectomy
9	F	72	CCC	Resection of IV-V liver segments
10	M	66	HCC	Resection of V-VI segments
11	F	67	HCC	Left hemihepatectomy
12	M	50	CRCM	Резекция II-III сегментов
13	F	69	CCC	Left hemihepatectomy
14	M	57	HCC	Resection of VI-VII segments

Table 1: Characteristics of patients with malignant liver tumors.

Thus, there were 5 cases of HCC, 4 cases of CCC, and 5 cases of CRCM.

Methodology of the study

Following a traditional laparotomy approach, the affected organ lobe was mobilized. A biopsy of the lesion tissue was performed. Tumor tissue fragments were collected from the tumor center and from liver tissue along the tumor periphery. Cryodestruction was then performed. A 50 mm diameter cryoapplicator was used (to cover the lesion and capture liver tissue). Over the course of 3–5 min, the applicator temperature was reduced to –180 to –187°C. Two applications with active freezing were performed (Figure 1a) with an exposure of 3 min and 1 min. After each application, the cryoapplicator was removed from the tumor tissue, and further warming of the destruction zone occurred spontaneously (Figure 1b). The cryodestruction technique didn't differ significantly in all patients, regardless of the localization of the tumor in the liver.

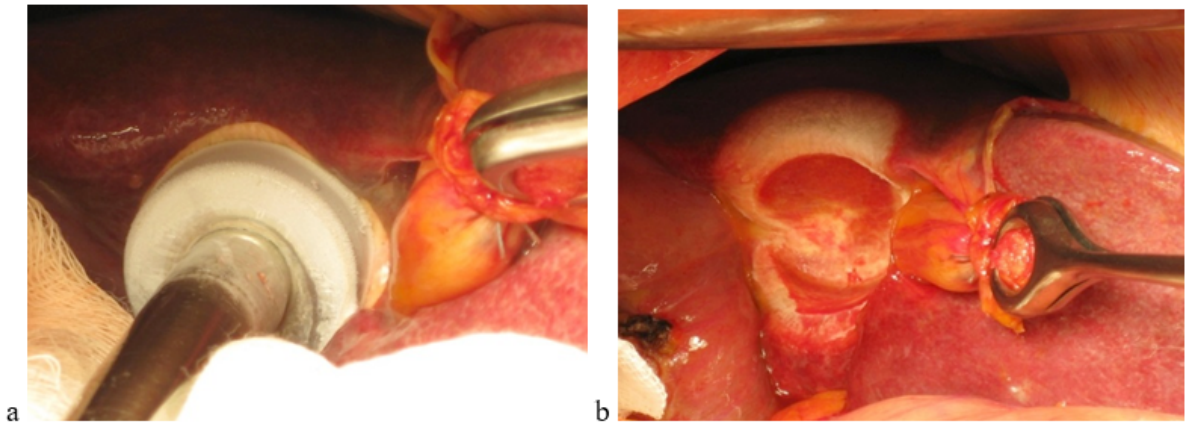

Figure 1: Stages of malignant liver tumors cryodestruction: active freezing (a), passive thawing (b).

During all stages of cryosurgery IOUS was performed (Fiure 2) to guide and monitor the process. For this purpose, an ultrasound system with intraoperative linear I- and T-shaped transducers with a power of 5 MHz was used. IOUS was used to determine the tumor center and place a cryogenic applicator directly in its projection. IOUS then allowed for the assessment of the formed "iceball" (the cryotherapy zone) and its mandatory extension into the surrounding liver parenchyma. The use of ultrasound guidance ensured adequate cryotherapy of the entire pathological node and avoided potential complications [24].

Figure 2: Ultrasound guidance during a malignant liver tumor cryodestruction. Active freezing stage.

Following the thermal exposure stage, a repeat biopsy of the lesion was performed to verify the results. Tumor tissue fragments were collected from the tumor center and from liver tissue along the periphery of the cryo-treated tumor. The collected material was promptly delivered to the pathology department without formalin treatment for subsequent electron microscopic examination of the tumor and its microenvironment. This analysis included morphometric analysis of the tumor, including an ultrastructural assessment of mitochondrial area in tumor cells before and after cryodestruction, as well as the detection of telocytes, followed by determination of the average number of microvesicles secreted by telocytes per 1 μm2 of extracellular matrix, as well as the extracellular matrix area (μm2). Morphometric analysis of mitochondria and microvesicles in tumor cells before and after cryodestruction was performed using the QuPath software. Statistical processing was performed in MS Excel and included calculations of the mean value of the indicators (M) and its standard deviation (Sd), as well as subsequent pairwise comparison within the group (before and after cryodestruction) using the Mann-Whitney test.

To conduct an electron microscopic examination of tumor tissue fragments in the early period (approximately 40-60 minutes) after cryotherapy, tumor pieces approximately 1 mm³ in size were fixed in a 2.5% glutaraldehyde solution and 1% osmium (VIII) oxide solution. The material was then dehydrated in alcohols at an increasing concentration gradient (50, 70, 96, and 100%), after which it was impregnated with a mixture of propylene oxide and araldite resin. After impregnation, the material was placed in capsules and embedded in araldite resin, then placed in an incubator at 60°C for two days. Image analysis and recording of light-optical preparations (section thickness 1.0-1.5 μm, stained with toluidine blue) were performed, and areas for ultratomy were precisely selected. Ultrathin sections (100–120 nm thick) were prepared on an ultramicrotome. The sections were stained with uranyl acetate and lead citrate and examined under an electron microscope in transmission mode at an accelerating voltage of 80 kV.

Results

During electron microscopic examination, ultrastructural signs of tumor cell cytodestruction were observed in the area directly exposed to the cryoapplicator. Most cells were completely destroyed and appeared as cellular debris. The integrity of the tumor cell plasma membrane was disrupted, making cell boundaries virtually indistinguishable. The state of cellular organelles also showed signs of destruction. Mitochondria were the most numerous organelles in tumor cells, so their damage and dysfunction led to the most severe destructive changes in the cells, including cell death.

Comparison of ultrastructural changes in HCC (Figure 3) and CRCM (Figure 4) cells after cryotherapy revealed similar changes, manifested in a complex of morphological alterations in the nucleus (deformation, wrinkling, compaction, and uneven, coarse chromatin condensation), characteristic of karyopyknosis and karyorrhexis—irreversible destructive processes. In HCC cells, the karyolemma was not visualized almost throughout its entire length, the nucleoplasm had a fine-granular appearance. Pronounced edema and homogenization of the cytoplasm, destruction of mitochondria and other organelles, did not allow differentiating mitochondria, which became an objective obstacle to conducting morphometric analysis (Figure 3). In CCC cells, pronounced destructive changes were noted, however, the ability to differentiate mitochondria after cryodestruction allowed for a comparative morphometric analysis of these organelles before and after cryotherapy (Figure 5). The average mitochondrial area in cells after cryodestruction was 0.48 ± 0.01 μm2 compared to the data before cryodestruction - 0.15 ± 0.02 μm2, i.e. it increased 3-fold ($p < 0.05$) (Table 2).

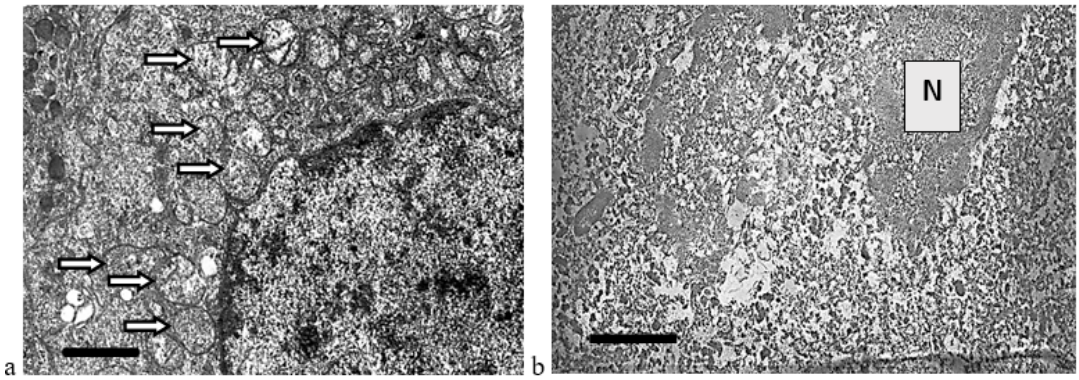

Figure 3: Destructive changes in HCC cells: a – tumor cell ultrastructure before cryodestruction, mitochondria – white arrow; b – devitalization of the malignant cell after cryodestruction; destruction of all intracellular organelles; homogenization of the nucleu (N); absence of nucleolemma, plasmalemma. The length of the scale line corresponds to 1 μm.

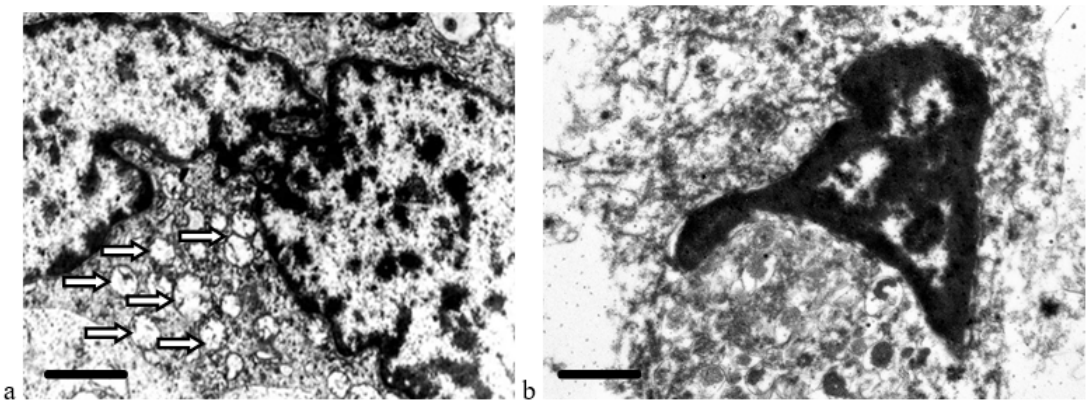

Figure 4: Destructive changes in CRCM cells: a – tumor cell ultrastructure before cryodestruction, mitochondria – white arrow; b – absence of plasma membrane, nucleolemma, destruction of intracellular organelles after cryotherapy. The scale line length corresponds to 1 μm.

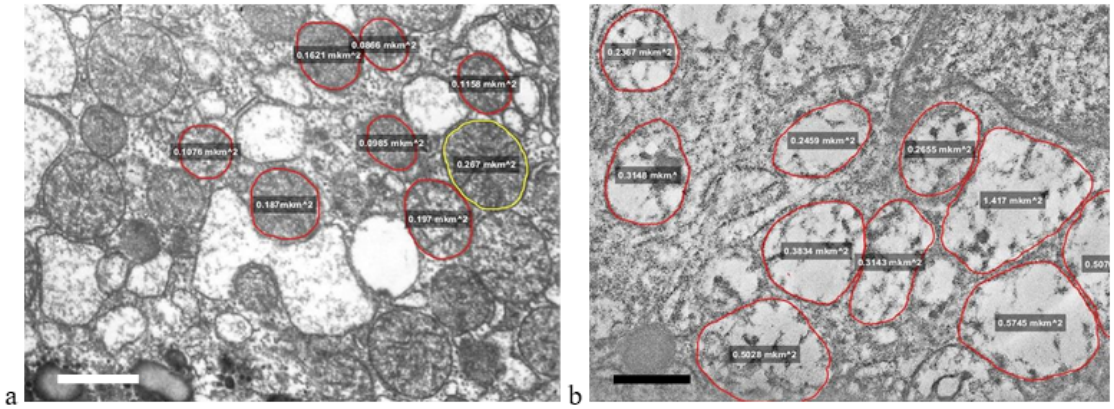

Figure 5: Destructive changes in CCC cells (mitochondria are circled and the area (μm^2) is indicated): a – tumor cell ultrastructure before cryodestruction; b – tumor cell ultrastructure after cryodestruction. The length of the scale line corresponds to 1 μm.

The relative preservation of mitochondrial ultrastructure in CCC may be explained by the resistance of ductal epithelial cells to external factors compared to more specialized cells such as hepatocytes or enterocytes. These biological properties are likely preserved during their neoplastic transformation, which is why HCC and CRCM cells are more sensitive to cryotherapy than CCC cells.

Against the background of destructive changes in tumor cells early after cryotherapy, changes were observed in the tumor stroma, which consists of an extracellular matrix containing collagen fibers, fibroblasts, and telocytes. Homogenization of collagen fibers with a loss of structure due to swelling was observed in the extracellular matrix, while the transverse striations characteristic of collagen fibrils completely disappeared (Figure 6b). Telopodiums of telocytes and altered fibroblasts were also visible among the altered collagen fibers. Lysis zones were observed in the electron-dense cytoplasm of fibroblasts; organelles were not detectable, and the cytolemma was fragmentarily absent. The fibroblast changes were irreversible (Figure 7b).

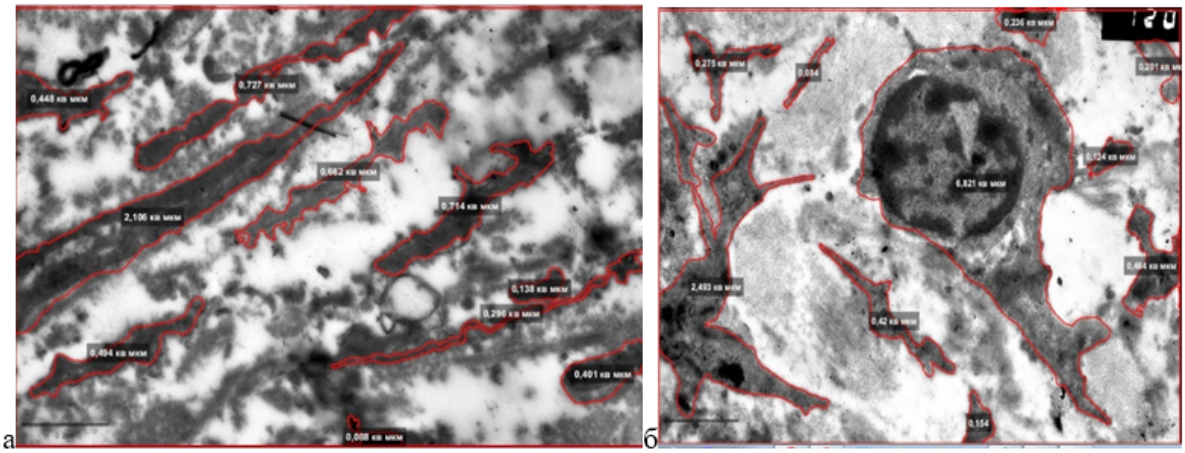

Figure 6: Destructive changes in the CCC stroma: a - before cryodestruction: fragments of electron-dense telopodiums; b - after cryodestruction: short electron-dense fragments of telopodiums. The area of the extracellular matrix and the number of microvesicles in it decreased slightly. The length of the scale line corresponds to 1 μm.

Telocyte nuclei were not visible in the fields of view selected for electron microscopic examination due to the structural features of the cells. Before cryotherapy, long telopodiums were observed between the tumor cells, containing mitochondria, profiles of the rough endoplasmic reticulum, cytoskeletal elements, caveolae, and microvesicles (Fig. 7a). After tumor cryodestruction, the cytoplasm in the telopodiums acquired a high electron density, areas of homogenization and lumpy structures were visible, while intracellular structures were not determined (Fig. 6b, 7b). Isolated microvesicles embedded in collagen fibers were noted near the telopodiums in the extracellular matrix. Expanded areas of the telopodiums, or podomas, were practically not observed. Rare homo- and heterocellular contacts (telocyte-telocyte; telocyte-fibroblast) were observed (Figure 7b).

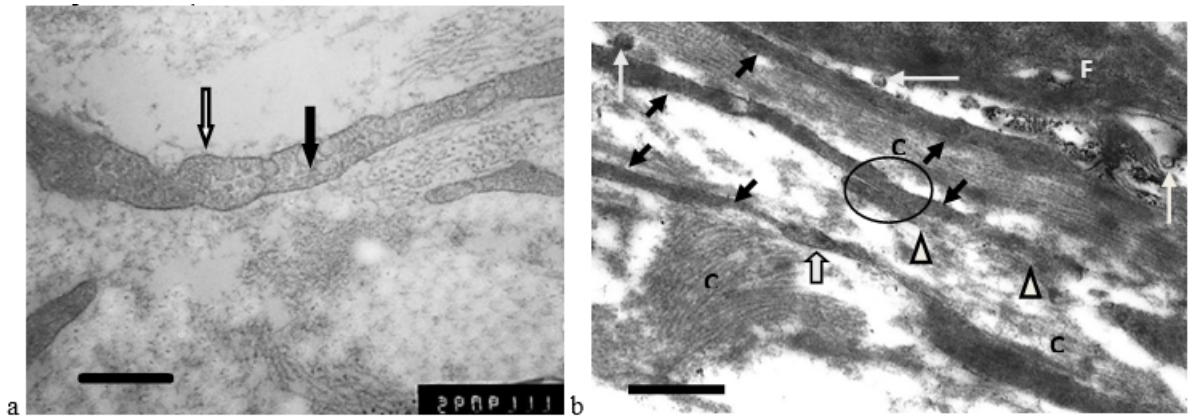

Figure 7: Destructive changes in the CRCM stroma: a – fragment (telopodia) of a telocyte before cryotherapy, microvesicles are determined in the cytoplasm (black arrow), caveolae (white arrow) are on the surface; b – after cryotherapy: among the swollen collagen fibers (C) there are electron-dense processes of telocytes (telopodia) (black arrows) and a destructively changed fibroblast (F). Single extracellular microvesicles (white arrow) are located near the telopodiums (areas of destroyed telopodiums – triangle; podome – wide white arrow; homocellular contact of telocytes – circle). The length of the scale line corresponds to 1 μm.

Summary information on the ultrastructural assessment of the tumor and its microenvironment before and after cryodestruction is presented in Table 2.

Tumor morphological variant	Tumor structures and their microenvironment		Cryotherapy	
			before	after
HCC	Telocytes	Number of microvesicles in 1 μm² extracellular matrix	1,23±0,06	Not visualized (cellular debris)
		Extracellular matrix area (μm²)	22,03±1,51	Cell boundaries are not defined
	Average area of one mitochondrion, μm²		0,17±0,03	Not visualized (cellular debris)
CCC	Telocytes	Number of microvesicles in 1 μm² extracellular matrix	1,64±0,04	1,28±0,07
		Extracellular matrix area (μm²)	30,43±2,01	24,18±1,60
	Average area of one mitochondrion, μm²		0,15±0,05	0,48±0,01*
CRCM	Telocytes	Number of microvesicles in 1 μm² extracellular matrix	1,33±0,06	0,46±0,03*
		Extracellular matrix area (μm²)	24,10±2,01	19,54±1,81
	Average area of one mitochondrion, μm²		0,10±0,01	0,35±0,11*
* — p ≤0,05 compared to data before cryodestruction.				

Table 2: Ultrastructural assessment of the tumor and its microenvironment before and after cryodestruction.

The presented data made it possible to develop a pathogenetically substantiated approach to the use of cryodestruction in the treatment of malignant liver tumors (HCC, CCC and CRCM) with confirmation of the effect on the tumor at the ultrastructural level (Table 3).

HCC		
Impact	effective	Destruction of mitochondria and extracellular matrix, the absence of microvesicles in the structure of HCC after cryotherapy indicate the effective implementation of destruction.
	ineffective	The presence of any of the elements (mitochondria, microvesicles, and extracellular matrix) in the HCC structure after cryotherapy indicates ineffective destruction. Additional cryotherapy is required (1st session – 3 minutes; 2nd session – 1 minute, or, if possible, surgical intervention).
CCC		
Impact	effective	A decrease in the structure of the CCC after cryotherapy of microvesicles by 30% or more, the extracellular matrix by 25% or more, an increase in the area of one mitochondrion by 30% or more indicates the effective implementation of destruction.
	ineffective	A decrease in the microvesicle structure by less than 30%, an increase in the extracellular matrix by less than 25%, or an increase in the area of a single mitochondrion by less than 30% after cryotherapy indicate ineffective destruction. Additional cryotherapy is required (1st session – 3 min; 2nd session – 1 min; 3rd session – 1 min, or, if possible, surgery).
CRCM		
Impact	effective	A decrease in the structure of CRCM after cryotherapy of microvesicles by 35% or more, the extracellular matrix by 80% or more, an increase in the area of one mitochondrion by 25% or more indicates effective destruction.
	ineffective	A decrease in the microvesicle structure by less than 35%, an increase in the extracellular matrix by less than 80%, or an increase in the area of a single mitochondrion by less than 25% after cryotherapy indicates ineffective destruction. Additional treatment is required (1st session – 3 minutes; 2nd session – 1 minute, or, if possible, surgery).

Table 3: Interpretation of cryodestruction results.

Thus, as a result of cryotherapy, ultrastructural signs of irreversible necrotic changes were observed in HCC and CRCM cells, as well as in the stroma, according to the data in Table 2. In CCC cells, pronounced dystrophic changes were observed early after cryotherapy. Relative stability of the intracellular structures of bile duct adenocarcinoma cells was noted compared to HCC and CRCM cells, indicating that tumors from highly specialized tissue were more sensitive to cryotherapy. This study allowed us to develop a new, pathogenetically substantiated approach to cryotherapy, including the frequency and duration of cryoapplications, depending on the tumor type and its histogenesis (Table 3).

A large number of telocyte processes and isolated fibroblasts were detected in liver tumors. Telocytes are known to regulate the interaction of organ parenchymal cells with the body by producing extracellular vesicles containing specific growth factors and microRNAs. Electron microscopic examination of liver tumor biopsies in the area of direct cryogenic exposure revealed ultrastructural signs of pronounced degenerative changes in tumor cells and stroma, particularly telocytes. Early changes in tumor cells after cryotherapy (approximately 40-60 minutes after exposure) were irreversible and manifested themselves in the disintegration of nuclear chromatin, destruction of the cytoskeleton, lysis of cell membranes, disruption of mitochondrial structure, and vacuolization of the cytoplasm. These data demonstrate the absolute necessity of "capturing" liver tissue around the tumor to interrupt potential translation chains and the spread of the tumor signal throughout the body.

Conclusion

A method for assessing the effectiveness of malignant liver tumor destruction following cryodestruction based on electron microscopic data has been developed. Electron microscopic examination of malignant liver tumor cells (HCC, BCC, and BCC) and the tumor microenvironment before and after cryodestruction allowed for the pathogenetic justification of a malignant tumor treatment regimen, confirming the tumor's destructive effect at the ultrastructural level.

References

1. Holbrook RF, Koo K, Ryan JA (1996) Resection of malignant primary liver tumors. Am J Surg 171: 453–455.
2. IshiiH., Furuse J, Kinoshita T, Konishi M, Nakagohri T, et al. (2008) Hepatectomy for hepatocellular carcinoma patients who meet the Milan criteria. Hepatogastroenterology 55:621–626.
3. Stucke K (2019) К вопросу о криохирургии печени: Материалы XXIV Международного конгресса хирургов. М 1972:202–204.

4. Alperovich BI, Merzlikin NV, Komkova TB (1992) Cryosurgical operations for diseases of the liver and pancreas. Khirurgiia 1992:104-7.

5. Revishvili ASh., Chzhao AV, Ionkin DA (2019) Cryosurgery. M.: GEOTAR-Media 2019; 376p.

6. Sumida S (1975) Frozen blood – Ten years of clinical experiences. Low Temp Med 1:7-14.

7. Sumida S, Eto S, Morishige F, Nakamura T, Sakai Y, et al. (1984) High-dose chemotherapy with frozen autologous marrow transplantation in patients with poor-prognosis tumors. Jpn J Clin Oncol 14:553-561.

8. Harada J, Miyasaka R, Sumida S (2004) Percutaneous cryotherapy of renal cell carcinoma under an open MRI system. Nova Science Publishers 3: 114p.

9. Kolck J, Schulze D, Bronnimann M, Furstner M, Fehrenbach U, et al. (2024) Percutaneous Cryoablation in the Liver: A Meta-Analysis and Review of Safety with a Focus on Incidence of Cryoshock and Major Complications. Cardiovasc Intervent Radiol 47:1471-1484.

10. Adam R, Akpinar E, Johann M, Kunstlinger F, Majno P, et al. (1997) Place of cryosurgery in the treatment of malignant liver tumors. Ann Surg 225:39-50.

11. Interventional radiology in oncology (development paths and technologies). Scientific and practical publication. Chief editors AM Granov and MI Davydov; edited by P.G. Tarazov and D.A. Granov, 2nd ed., supplemented. St Petersburg FOLIO 2013; 560 p.

12. Niu LZ, Li JL, Xu KC (2014) Percutaneous Cryoablation for Liver Cancer. J Clin Transl Hepatol 2:182-188.

13. Crocetti L, de Baére T, Pereira PL, Tarantino FP (2020) CIRSE Standards of Practice on Thermal Ablation of Liver Tumours. Cardiovasc Intervent Radiol 43:951-962.

14. Soto AM, Sonnenschein C (2011) The tissue organization field theory of cancer: a testable replacement for the somatic mutation theory. Bioessays 33:332-340.

15. Popescu LM, Faussone-Pellegrini MS (2010) TELOCYTES - a case of serendipity: the winding way from Interstitial Cells of Cajal (ICC), via Interstitial Cajal-Like Cells (ICLC) to TELOCYTES. J Cell Mol Med 14:729-740.

16. Dymshits GM (2002) Surprises of the mitochondrial genome. Priroda 6:54–61.

17. Hahn A, Zuryn S (2018) The Cellular Mitochondrial Genome Landscape in Disease. Trends Cell Biol 29:227-240.

18. Lim K (2024) Mitochondrial genome editing: strategies, challenges, and applications. BMB Rep 57:19-29.

19. Usoltseva NV, Usoltseva VA (1980) Liquid crystalline state and metabolism. Priroda 12:56–62.

20. Shafranov VV, Borkhunova EN, Tsyganov DI, Torba AI, Taganov AV, et al. (2013) Modern concept of biological tissue destruction during local cryodestruction. Humanitarian Bulletin 12:142.

21. Smythies J (2015) Intercellular Signaling in Cancer – the SMT and TOFT Hypotheses, Exosomes, Telocytes and Metastases: Is the Messenger in the Message? J Cancer 6:604-609.

22. Chzhao AV, Chekmareva IA, Paklina OV, Ionkin DA, Kalinin DV, et al. (2017) Early Morphological Changes of Hepatocytes After Cryodestruction. Journal of Anatomy and Histopathology 6:109-114.

23. Yang WL, Addona T, Nair DG, Qi L, Ravikumar TS (2003) Apoptosis induced by cryo-injury in human colorectal cancer cells is associated with mitochondrial dysfunction. Int J Cancer 103:360-369.

24. Stepanova Yu A, Ionkin DA, Zhavoronkova OI, Chzhao AV, Vishnevsky VA (2023) Intraoperative ultrasound examination of colorectal cancer metastases to the liver. Bulletin of Experimental and Clinical Surgery 16:167-179.